Collapse and Rebound of a Gas Bubble

By Guillermo H. Goldsztein

In this paper, we study the collapse and rebound of a gas bubble. Our goals are twofold: (1) we want to stress that different mathematical models may lead to extremely different results and (2) we introduce a new class of simplified reliable models. We accomplish our first goal by showing that the results obtained from two of the simplest and most widely used models (the isothermal and adiabatic approximations) are very different while the bubble is highly compressed. This period of time is short but it is of crucial importance in most phenomena where bubble collapses are relevant. To accomplish our second goal, we identify a nondimensional parameter that is a quantification of the strength of the bubble collapse and we show how to use this large parameter to obtain new simplified models through the use of standard asymptotic techniques. Illustrative examples and discussions on the wide range of applicability of the approach introduced in this work are given.

1. Introduction

In this paper, we study the *collapse and rebound of a gas bubble*. To describe the phenomenon to which this expression makes reference to, consider the following situation. A gas bubble is immersed in a liquid. The pressure in the liquid becomes and remains negative for enough time for the bubble to grow many

Address for correspondence: G. H. Goldsztein, School of Mathematics, Georgia Institute of Technology; Atlanta, GA 30332-0160; e-mail: ggold@math.gatech.edu

STUDIES IN APPLIED MATHEMATICS 112:101–132

Published by Blackwell Publishing, 350 Main Street, Malden, MA 02148, USA, and 9600 Garsington Road, Oxford, OX4 2DQ, UK.

times its equilibrium size. Once the bubble has expanded, the pressure in the liquid increases to a positive value. As a consequence, the bubble (if it still exists) decreases in size violently, overshooting its equilibrium size and bouncing back (whenever it does not break). This process is usually referred to as the collapse and rebound of the bubble.

Bubble collapses are frequently found in practice and easy to produce. Cavitation damage, sonochemistry, shock wave lithotripsy, ultrasonic imaging, and sonoluminescence are examples of technological and scientific importance where bubble collapses play a central role.

Cavitation damage makes reference to the phenomenon that can be described as follows. Strong pressure variations in the liquid are produced by the jet and the shock emitted after the bubble collapses. The combined effect of several bubbles undergoing this process is believed to cause erosion in nearby solids (see [4, 23, 53]). This is an undesirable effect.

During a strong collapse, bubbles emit light. This phenomenon is known as sonoluminescence. This light emission is believed to be due to chemical reactions induced by the extremely high temperatures attained inside the bubble during its compression. Multi-bubble sonoluminescence was observed over half a century ago (see [4, 11, 32, 52, 53]), but it was the most recent discovery of single bubble sonoluminescence that sparked a lot of interest within the scientific community (see [1–3, 5, 12, 13, 16, 46]).

Chemical reactions result from the high temperatures and pressures in the bubble during the collapse. This phenomenon is known as sonochemistry and has a wide variety of applications (see [27, 28, 49]).

It is clear that any successful quantitative theory that describes any of the phenomena mentioned above, should be able to predict the dynamics of the collapse and rebound of a bubble. A large number of different mathematical models to study the dynamics of single spherical bubbles can be found in the literature. These models range from simple ODEs (Rayleigh–Plesset equations) to complex systems of PDEs (Navier–Stokes equations). Some of the main contributions to the field of bubble dynamics include [7–10, 33–41, 43, 45, 47].

Whenever we consider phenomena in which bubble collapses are relevant, we are faced with the dilemma of choosing an appropriate model. On one hand, we would like to use a model that can be easily implemented and produces results easy to interpret. On the other hand, we would like to make sure that no important physical effects are neglected by our model so that the results we obtain are reliable. In this paper, we address some of these issues.

The goals of the present work are twofold. Our first goal is to stress that different models can lead to extremely different results. On the other hand, we note that the bubble collapse is a violent and fast motion. This violence of the collapse can be quantified with a large non-dimensional parameter that we identify. Our second goal is to show that asymptotics on this parameter is a reliable source of new simplified models.

To keep our analysis as simple as possible, we will assume that the liquid under consideration is incompressible and inviscid, the gas inside the bubble is inviscid, the mach number inside the bubble and the effect of surface tension are negligible and the system posses spherical symmetry.

Some of the physical effects neglected in this paper become important in the short period of time while the bubble is compressed. For example the compressibility of the liquid slows down the speed at which the bubble collapses. Thus, if our goal is to accurately predict the value of different variables such as temperature or pressure during the collapse, the analysis to be presented here has to be extended to include some of the physical effects mentioned and possibly others.

However, the exact values of the variables in the short period of time while the bubble is compressed is not always the goal pursued. An example is given in Section 5, where the goal is to find the applied sound field that, while satisfying certain restrictions, maximizes the strength of the collapse. The model presented here leads to the correct result when applied to this example.

The objective of this work is to show how to obtain a dimensionless large parameter that quantifies the strength of the collapse and how to use it to obtain reduced models. Thus, to keep the analysis as clear as possible we have chosen to make the physical assumptions mentioned above. We remark that part of the value of this analysis is that it can be extended to include physical effects neglected here (such as liquid compressibility). These extensions are currently being developed.

We will study a system consisting of a single gas bubble immersed in a liquid that extends to infinity. To model the bubble collapse and rebound, we will simply study the evolution of this system when the initial radius $R(0)$ is much larger than the radius at equilibrium conditions R_e ($R(0) \gg R_e$), the initial velocity of the bubble wall is 0 ($R_t(0) = 0$) and the pressure in the liquid far away from the bubble remains at all times equal to the equilibrium pressure p_e. Under these conditions, the bubble behaves as follows. Because $R(0) \gg R_e$, the pressure inside the bubble at time $t = 0$ is smaller than the pressure in the liquid far away from the bubble p_e. As a consequence, the bubble size starts to decrease. Because much inertia is gained, the bubble overshoots its equilibrium size becoming very small. Once enough pressure inside the bubble builds up due to compression, its size stops decreasing and starts to increase. This motion occurs in two different time scales. Most of the time the bubble is expanded and for a much shorter time the bubble is compressed. Figure 1 of section 2 shows a typical plot of R versus t under the present conditions.

To describe the evolution of this system, it is necessary to determine the pressure inside the bubble. In this regard, the polytropic approximation has been widely used by models in the literature. More precisely, the pressure inside the bubble is assumed by these models to be proportional to $R^{-3\kappa}$, where κ is a constant. In particular, $\kappa = 1$ corresponds to the isothermal approximation (i.e.,

the temperature in the bubble is constant in both space and time) and $\kappa = \gamma$ (γ being the ratio of the specific heats of the gas) corresponds to the adiabatic approximation (i.e., the entropy in the bubble is constant along particle paths).

In Section 2 we will use both the isothermal and the adiabatic approximation in our modeling of the bubble collapse and rebound. We will show that both approximations give very similar results while the bubble is expanded (which is for most of the time). In fact, the curves R versus t obtained by both approximations are indistinguishable to the naked eye when plotted in the time scale that the bubble takes to go from its maximum size to its minimum size (see Figure 1). This plot can mislead to wrong conclusions because, by looking at it, one could be tempted to believe that both approximations give the same results and they are both correct. However, sometimes we are particularly interested in the behavior of the system during the short period of time that the bubble is compressed. For example, if we are modeling the phenomenon of sonoluminescence, we might want to predict the temperatures attained inside the bubble. Thus, a look at Figure 1 is not enough to draw any conclusions. In fact, we will show in Section 2 that the results obtained from these two approximations are extremely different for a short period of time while the bubble is compressed (see Figure 2).

This discrepancy rises the following question: which one of these two approximations (if anyone) is giving us the correct results? To answer this question, we note that the gas is isothermal while the bubble is expanded, but as the bubble collapses, this approximation eventually breaks down. In fact, the gas is adiabatic while the bubble is compressed. Thus, each approximation is valid during different periods of time but neither is valid at *all* times. This behavior suggests the use of the isothermal approximation while the bubble is expanded and the adiabatic approximation while the bubble is compressed. In Section 3, we prescribe an *informal* approach following these ideas. We say that this procedure of Section 3 is informal because we use an ad-hoc rule to decide when the motion ceases to be isothermal and becomes adiabatic. However, the presentation of this analysis is justified because it is simple and it introduces some of the main ideas behind the more *formal* procedure that is presented later in this work.

In Section 4 we undertake a more formal analysis. Our starting point is the complete set of PDEs (conservation of mass, momentum, and energy both in the liquid and the gas). As it has been recognized independently by two different groups (see [30, 31] and [43, 42]), under the conditions we consider in this work, this complete set of equations can be reduced to a nonlinear PDE coupled with the Rayleigh–Plesset equation. We nondimensionalize these equations and observe that two parameters characterize our problem. One of them can be considered a measure of the strength of the collapse and the other one is the nondimensional coefficient of thermal diffusion inside the bubble. We profit from the fact that the first of these two parameters is large to simplify

the system with the use of asymptotic techniques (boundary layers in time). As a result we split the time domain in three. While the bubble is expanded, it behaves isothermally and the dynamics of the bubble radius is not affected by the pressure in the gas. As the bubble becomes small, we need to introduce a boundary layer in time where the isothermal approximation is no longer valid. Eventually, once the bubble becomes small enough, the evolution of the bubble radius is affected by the high pressures inside the bubble. Thus, a new boundary layer (inside the one we already had) develops. There, the gas is adiabatic.

The value of our analysis becomes clear when we compare our approach with computing the evolution of the system numerically without the use of asymptotics. A first advantage of our approach is that its results are easier to interpret. More precisely, the dependence of the solution as a function of the nondimensional parameters of the system (the strength of the collapse and the coefficient of thermal diffusion in the bubble) is explicitly shown. This is not surprising because the result of the use of asymptotic techniques is to reduce the original system to simpler systems that do not contain the expansion parameters. Another advantage of our method is that it is computationally cheaper. Our simplified model requires the solution of two ODEs and the computation of a constant. The computation of this constant requires the numerical solution of a simple PDE. These equations are very inexpensive to solve and they do not depend on the parameters of our original system. On the other hand, performing numerical computations on the original system becomes extremely expensive as the collapse becomes stronger. (Two are the reasons for this increase in computational times. The first one is the presence of different time scales in the problem. The difference in these time scales increases with the strength of the collapse. The second reason is that the thickness of the boundary layer in space developed inside the bubble while it is compressed decreases as the strength of the collapse increases.) As an example supporting our discussion, we mention that the authors of [19] were faced with these difficulties to resolve the bubble collapse numerically in their study of single bubble sonoluminescence. As a consequence, they had a limit on the size of the forcing sound amplitude that they could use in their numerical computations. Our approach does not have these limitations. In fact, the problem studied in [19] is a typical example where our method can be used.

In Section 5 we show that our approach can be used in any situation involving bubble collapses (not just in the examples presented in this paper). In this regard, we mention that our asymptotic analysis could be a component of a numerical code that simulates the dynamics of a system composed of one or several bubbles in a liquid. This code would detect when a bubble is collapsing, use our asymptotic results and then continue the numerical calculation after the rebound, avoiding the computationally expensive task of resolving the bubble collapse numerically. In Section 5 we also present two illustrative examples. In the first example the system is initially in equilibrium.

Suddenly, at time equal 0 $t = 0$, the pressure in the liquid away from the bubble p_∞ becomes negative and remains constant for a period of time $[0, t_0]$. This period of time is long enough so that the bubble size at $t = t_0$ is many times its equilibrium value. At this time $t = t_0$, the pressure p_∞ becomes positive again. In our second example, the pressure away from the bubble p_∞ is not constant but is of the form $p_\infty = p_e(1 + a \sin(\omega t) + b \sin(2\omega t + \phi))$, where p_e is the equilibrium pressure. We use our method to find the constants a, b, and ϕ that maximize the strength of the bubble collapse under the condition that the acoustic intensity and frequency are constant (i.e., $a^2 + b^2$ and ω are constants). These two examples illustrate the general applicability and some of the advantages of our method.

Bubble collapses are sometimes desirable. In sonochemistry for example, chemical reactions are produced by the extremely high temperatures generated in the interior and in the vicinity of bubbles when they collapse. In these situations, bubble collapses are induced by ultrasound. Clearly, it is desirable to be able to induce bubble collapses with low acoustic intensities. Efforts in this direction have been undertaken (see [17, 20, 50] for example). In particular, the objective of the work in [20, 50] is to develop a sonodynamic approach to cancer therapy. These authors found experimentally that the acoustic intensity required to produce some chemical reactions can be much lower if the ultrasound has two frequency components instead of one. This work is the motivation of our second example of Section 5.

To conclude the introduction we mention that while a large number of studies on the dynamics of collapsing bubbles exists (including the works previously mentioned and [14, 18, 21, 22, 24–26, 29, 42–44, 48, 51]), the analysis introduced here is new and will lead to new simplified and reliable models.

2. The polytropic approximations

In this Section we will use both the adiabatic and the isothermal approximations and we will compare the results obtained.

Here and in the rest of this paper, we assume that the liquid is incompressible and inviscid, the gas inside the bubble is ideal and inviscid, the effect of surface tension is negligible, the mach number inside the bubble is negligible (i.e., the bubble wall speed is much smaller that the sound speed inside the bubble), and the system possesses spherical symmetry. Under these conditions, the evolution of a gas bubble immersed in a liquid that extends to infinity is described by the Rayleigh–Plesset equation

$$\rho_\ell \left(R R_{tt} + \tfrac{3}{2} R_t^2 \right) + p_\infty(t) = p(t) \tag{1}$$

where ρ_ℓ is the density of the liquid, R is the radius of the bubble, t is the time, $p_\infty(t)$ is the pressure in the liquid at infinity, and $p(t)$ is the pressure at

the bubble wall on the side of the gas. This equation was first obtained by Rayleigh (see [47]) and its derivation can be found in many books on bubble dynamics (see [4, 53]).

In this Section we also assume that the gas is polytropic (i.e., the pressure is proportional to a power of the density), which, under the present conditions, implies

$$p(t) = cteR^{-3\kappa} \tag{2}$$

for some constant *cte*. Equation (2) reduces to the isothermal approximation when $\kappa = 1$ and to the adiabatic approximation when $\kappa = \gamma$ (γ being the ratio of the specific heats of the gas). If the gas is isothermal and the temperature is the equilibrium temperature, the constant *cte* in Equation (2) is given by $p_e R_e^3$ (where p_e and R_e are the pressure and bubble radius at equilibrium conditions, respectively). If the gas is adiabatic, the constant *cte* depends on the total amount of entropy inside the bubble. In other words, this constant depends on the initial conditions. Following most models in the literature, we choose $cte = p_e R_e^{3\gamma}$ if $\kappa = \gamma$.

To model the bubble collapse and rebound, we assume the pressure far away from the bubble to be equal to the equilibrium pressure, the initial radius to be much larger than the equilibrium radius, and the initial bubble wall velocity to be 0. Thus, we are interested in the solutions of the system

$$\rho_\ell \left(RR_{tt} + \frac{3}{2} R_t^2 \right) + p_e = p_e \left(\frac{R_e}{R} \right)^{3\kappa} \qquad R(0) = R_0 \text{ and } R_t(0) = 0\,, \tag{3}$$

where $R_0 \gg R_e$, for $\kappa = 1$ and $\kappa = \gamma$. In our calculations we have chosen $R_0 = 10R_e$ and $\gamma = 1.4$ (these values are commonly found in practice). Figure 1 shows the two curves R/R_e versus t/t_e obtained with the adiabatic and isothermal approximations. The constant t_e is the natural time scale

$$t_e = R_e \sqrt{\frac{\rho_\ell}{p_e}}. \tag{4}$$

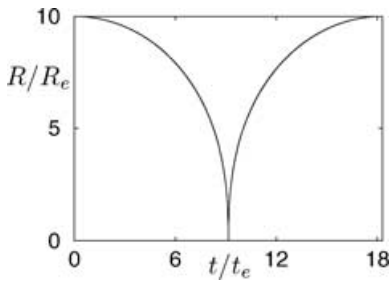

Figure 1. Plots of R/R_e versus t/t_e obtained with both the isothermal and the adiabatic approximations. The two curves are indistinguishable.

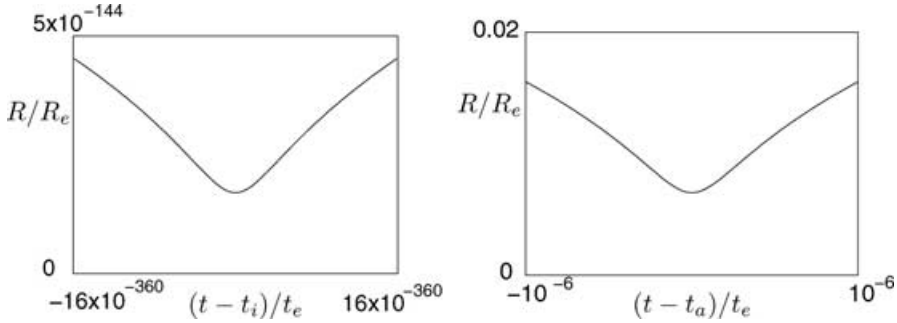

Figure 2. A closer look at the plots R/R_e versus t/t_e (with the origin of the horizontal axis shifted) corresponding to the isothermal (left figure) and the adiabatic (right figure) approximations for times where the radius is close to its minimum value. R attains its minimum at $t = t_i$ and $t = t_a$ when the isothermal and adiabatic approximations are used, respectively.

These curves looked like one. They are indistinguishable to the naked eye. However, a closer look at these curves reveals that these approximations give extremely different results for a short period of time while the radius is close its minimum (see Figure 2). This disagreement applies not only to the bubble radius R but also to the other variables in the problem (temperature, pressure, velocity, etc.).

A more precise quantification of the discrepancy between these approximations can be easily obtained. In Appendix A we show that the asymptotic behavior of $R_{\min}$ (the minimum of R) as δ, the ratio between the equilibrium and the initial radius

$$\delta = \frac{R_e}{R_0}, \tag{5}$$

becomes small, is given by

$$R_{\min} \approx \frac{R_e}{\delta} \exp\left(-\frac{1}{3\delta^3}\right) \quad \text{or} \quad R_{\min} \approx \frac{R_e}{(\gamma-1)^{\frac{1}{3(\gamma-1)}}} \delta^{\frac{1}{\gamma-1}} \tag{6}$$

depending whether the isothermal or the adiabatic approximation is used, respectively. Thus, evaluating these expressions at $\delta = 0.1$ and $\gamma = 1.4$, we obtain that $R_{\min} \approx 1.7 \times 10^{-144} R_e$ and $R_{\min} \approx 6.8 \times 10^{-3} R_e$ in the isothermal and the adiabatic case, respectively.

In the class of phenomena that motivates the present study (cavitation damage, sonoluminescence, sonochemistry, etc.), we are particularly interested in the behavior of the system while the bubble is compressed. In this regard, the calculations of this section show that different models can lead to extremely different results.

3. Failure of the polytropic approximations: An informal solution

The disagreement found between the isothermal and the adiabatic approximations raises doubts on their validity. In this section we address this issue and we prescribe an informal procedure to describe the evolution of the bubble. The purpose of this section is to gain insight on the behavior of our system and to introduce the main ideas of the more formal asymptotic analysis of Section 4.

3.1. Thermal diffusion time scale

We start by discussing the criteria of the validity of the isothermal and adiabatic approximations. To this end, we need to consider the energy equation inside the bubble, which, under our present conditions, takes the form

$$c_v \rho (T_t + v T_r) + \frac{(r^2 v)_r}{r^2} p = \frac{\left(\lambda r^2 T_r\right)_r}{r^2}, \tag{7}$$

where ρ is the density of the gas, T its temperature, v its velocity, λ its thermal conductivity, c_v its specific heat at constant volume, and r is the radial spatial variable (i.e., the distance to the center of the bubble). We assume that both c_v and λ are constants. Making use of the estimates

$$\frac{\partial}{\partial r} = O(R^{-1}) \quad \text{and} \quad \rho = O\left(\rho_g R_e^3 R^{-3}\right), \tag{8}$$

where ρ_g is the density of the gas at equilibrium conditions, we obtain (comparing the first term of (7) with its right-hand side) the thermal diffusion time scale

$$t_d = \frac{c_v \rho_g R_e^3}{\lambda R}. \tag{9}$$

Thus, the gas is isothermal while any other time scale in the problem is much larger than t_d, and it behaves adiabatically for any period of time much shorter that t_d. Note that the thermal diffusion time scale depends on the bubble size $t_d = t_d(R)$.

3.2. An informal model for the bubble evolution

We now go back to our description of the bubble collapse and rebound (i.e., the solution of (1) with $p_\infty(t) = p_e$ and initial conditions $R(0) = R_0 \gg R_e$ and $R_t(0) = 0$). While the bubble is expanded, the pressure in the gas is small and as a consequence, it does not affect the evolution of the bubble radius. Accordingly, $p(t)$ can be initially neglected from Equation (1). Thus, we replace our system (1) by

$$\rho_\ell \left(R R_{tt} + \tfrac{3}{2} R_t^2\right) + p_e = 0 \qquad R(0) = R_0 \quad \text{and} \quad R_t(0) = 0. \tag{10}$$

The solution $R(t)$ of this equation decreases monotonically and it becomes 0 at a finite time t_c. In fact, the asymptotic behavior of R as t approaches t_c is given by

$$R \sim A R_e t_e^{-\frac{2}{5}} (t_c - t)^{\frac{2}{5}} \qquad \text{with} \quad A = \left(\frac{25}{6}\right)^{\frac{1}{5}} \delta^{-\frac{3}{5}}, \tag{11}$$

where t_e and δ were introduced in (4) and (5), respectively. This asymptotic formula is due to Rayleigh (see [47]) and its derivation is given in the Appendix B.

As the bubble decreases in size, the pressure in the gas increases. Thus, once the bubble is small enough, this built up in pressure affects the evolution of our system preventing the bubble radius to become 0. As a consequence, the assumption under which Equation (10) was obtained ($p(t)$ being negligible) is no longer valid. This implies that, for a period of time while the bubble is compressed, we cannot neglect the pressure inside the bubble. To evaluate $p(t)$, we should, in principle, integrate the energy Equation (7) coupled with the Rayleigh–Plesset Equation (1). To avoid this and motivated by our knowledge of the qualitative behavior of our system, that is, the motion is isothermal while the bubble is expanded and adiabatic while the bubble is compressed, we prescribe the following rule.

3.2.1. *Rule.* We use the isothermal approximation in the time interval $[0, t_\alpha]$ and the adiabatic approximation in $[t_\alpha, t_{\min}]$, where $t_{\min}$ denotes the time at which R attains its minimum and t_α is determined next.

To select t_α, we argue as follows. We expect that $p(t)$ affects the evolution of our system for a period of time so small that the following assumption holds:

ASSUMPTION 1: *The effect of $p(t)$ on $R(t)$ is negligible in the time interval $[0, t_\alpha]$.*

Accordingly, we take R to be the solution of (10) in $[0, t_\alpha]$. On the other hand, we expect that the bubble decreases in size substantially before the isothermal approximation fails and thus, we expect that the following assumption is also valid:

ASSUMPTION 2: *Equation (11) is valid at $t = t_\alpha$.*

Now the choice of t_α is natural, namely, because the characteristic time scale of (10) is $t_c - t$, the isothermal approximation fails when $t_c - t$ is not much larger than the thermal diffusion time scale t_d (see (9)), thus, we take t_α to be the solution of

$$t_c - t_\alpha = t_d(R(t_\alpha)), \tag{12}$$

where t_d is given by (9) and R is given by (11). Once we solve (12), we have

$$t_\alpha = t_c - \left(\frac{6}{25}\right)^{\frac{1}{7}} t_e \mu^{-\frac{5}{7}} \delta^{\frac{3}{7}}, \tag{13}$$

where μ denotes the nondimensional coefficient of thermal diffusion inside the bubble

$$\mu = \frac{\lambda}{c_v \rho_g R_e} \sqrt{\frac{\rho_\ell}{p_e}}. \tag{14}$$

Having chosen t_α, it only remains to prescribe $p(t)$ in the time interval $[t_\alpha, t_{\min}]$. According to our *rule*, the gas behaves adiabatically during this period of time and thus, the pressure inside the bubble is given by

$$p(t) = CR(t)^{-3\gamma} \quad \text{if} \quad t \in [t_\alpha, t_{\min}] \tag{15}$$

for some constant C. To compute this constant C we simply require the pressure $p(t)$ to be continuous at $t = t_\alpha$. Thus, because our *rule* assumes the isothermal approximation ($p(t) = p_e(R_e/R)^3$) for $t < t_\alpha$ and Equation (15) for $t > t_\alpha$, we have

$$p = CR^{-3\gamma} = p_e \left(\frac{R_e}{R}\right)^3 \quad \text{at} \quad t = t_\alpha, \tag{16}$$

from where C can be easily computed once R is replaced by its asymptotic approximation (11)

$$C = \left(\frac{25}{6}\right)^{\frac{3}{7}(\gamma-1)} \delta^{-\frac{9}{7}(\gamma-1)} \mu^{-\frac{6}{7}(\gamma-1)} p_e R_e^{3\gamma}. \tag{17}$$

To conclude our informal description of the bubble collapse and rebound, we should verify the Assumptions 1 and 2. In this regard, we note that a typical value of μ (corresponding to the liquid being water, the gas being air, the equilibrium radius, temperature and pressure being 10 μm, 300 K and 1 atm respectively) is 0.5. Thus, we assume that μ is a parameter of order 1, and as a consequence, because δ is small, we have that Equation (13) implies that $t_c - t_\alpha \ll t_c$ (because $t_c = O(\delta^{-1} t_e)$), which confirms the validity of Assumptions 2. On the other hand, to verify assumption 1, we note that it is only necessary to confirm this assumption at $t = t_\alpha$ which can be easily done using the asymptotic formula for R (Equation (11)).

3.3. Summary and characteristics of the informal model

In summary, according to the method presented in this section, the bubble radius R is given by

$$R(t) = \begin{cases} R_i(t) & \text{if} \quad 0 \le t \le t_\alpha, \\ R_a(t) & \text{if} \quad t_\alpha \le t \le t_{\min}, \end{cases} \tag{18}$$

where t_α was defined in (13), $t_{\min}$ is the time at which $R_a(t)$ attains its minimum, $R_i(t)$ is the solution of (10) and $R_a(t)$ is the solution of

$$\rho_\ell\left(R_a R_{att} + \tfrac{3}{2}R_{at}^2\right) + p_e = C R_a^{-3\gamma}, \tag{19}$$

with C given by (17) and (because (11) is valid at $t = t_\alpha$) the initial conditions to integrate (19) are

$$R_a(t_\alpha) = A R_e t_e^{-\frac{2}{5}}(t_c - t_\alpha)^{\frac{2}{5}} \quad \text{and} \quad R_{at}(t_\alpha) = -\tfrac{2}{5} A R_e t_e^{-\frac{2}{5}}(t_c - t_\alpha)^{-\frac{3}{5}} \tag{20}$$

(where A is given in (11)). Note that given our conditions, we have $R(2t_{\min} - t) = R(t)$ for any $0 \le t \le t_{\min}$.

The nondimensional parameters of our system are δ defined in (5), and the nondimensional thermal diffusion coefficient inside the bubble μ, which was introduced in (14). Figure 3 shows a plot of R/R_e versus t/t_e (R given by (18))

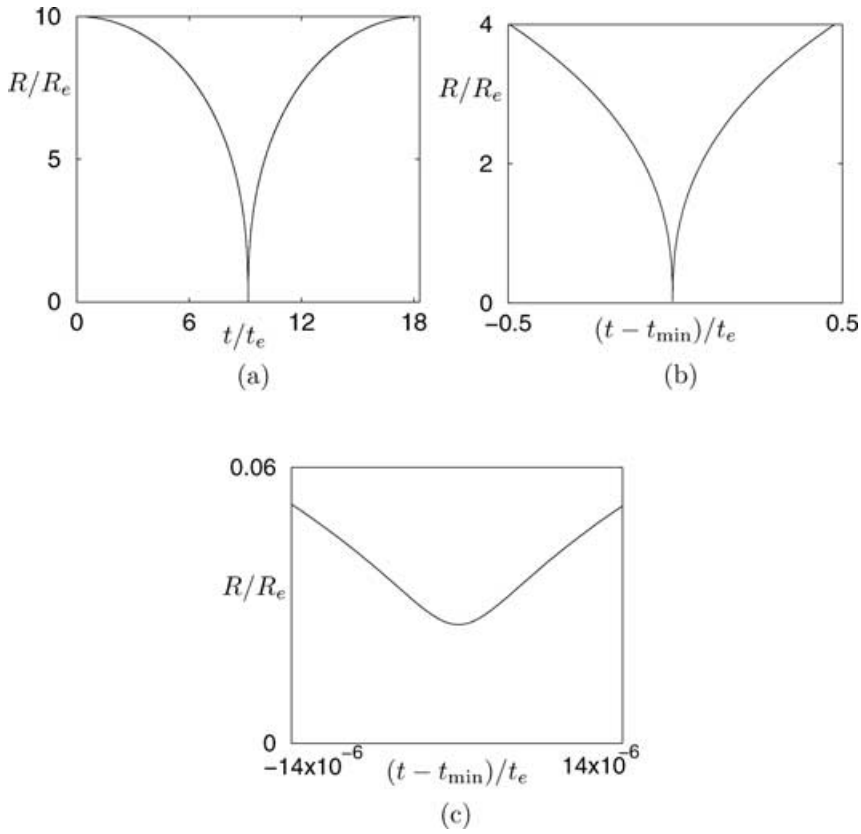

Figure 3. Plots R/R_e versus t/t_e corresponding to $\delta = 0.1$, $\gamma = 1.4$, and $\mu = 0.5$ obtained by Equation (18).

with $\delta = 0.1$, $\mu = 0.5$, and $\gamma = 1.4$. As expected, the plot in Figure 3(a) looks exactly like the one in Figure 1. The time range of the plot in Figure 3(b) is $[t_\alpha, 2t_{\min} - t_\alpha]$. During this period our present model assumes the adiabatic approximation. The plot in Figure 3(c) shows a closer look of the curve R/R_e versus t/t_e around the time where the radius attains its minimum. These plots clearly indicate the presence of three different time scales: (1) most of the time the gas inside the bubble is isothermal and its pressure does not affect the radius evolution (Figure 3(a)); (2) the time interval $[t_\alpha, 2t_{\min} - t_\alpha]$, where the isothermal approximation fails (Figure 3(b)); and (3) a shorter period of time where the pressure inside the bubble affects the dynamics of the radius (Figure 3(c)).

To compare the results of this approach with the ones obtained in the previous section, we remind that the values of the minimum radius are $R_{\min} \approx 1.7 \times 10^{-144} R_e$ and $R_{\min} \approx 6.8 \times 10^{-3} R_e$ when the isothermal and adiabatic approximations are used, respectively (with $\delta = 0.1$ and $\gamma = 1.4$). On the other hand, we show in Appendix C that the asymptotic behavior of $R_{\min}$ as $\delta \to 0$ according to the present model is

$$R_{\min} \approx R_e \left(\frac{25}{6\mu^2} \right)^{\frac{1}{7}} \frac{1}{(\gamma - 1)^{\frac{1}{3(\gamma-1)}}} \delta^{\frac{1}{\gamma-1} - \frac{3}{7}}. \tag{21}$$

Thus, for the example under consideration ($\delta = 0.1$, $\gamma = 1.4$, and $\mu = 0.5$), we have $R_{\min} \approx 0.027 R_e$.

We end this section with some comments. Although our rule to compute the pressure inside the bubble is not a formally correct approximation, our results have the right order of magnitude (this will be confirmed later in this paper). Finally, we mention that two key characteristics of our system make possible the present analysis and its more formal version that will follow, namely, δ is a small parameter and the transition from isothermal to adiabatic motion occurs while the pressure inside the bubble $p(t)$ does not affect the dynamics of the radius $R(t)$.

4. Formal asymptotic analysis

In this section we undertake a more formal analysis of the bubble collapse and rebound. We will first present the system of equations that govern the evolution of our system, then we will solve this system with the use of asymptotic techniques, and finally we will discuss some of the characteristics of the solution obtained.

4.1. Governing equations

We assume that the liquid under consideration is incompressible and inviscid, the gas inside the bubble is ideal and inviscid, the mach number inside the

bubble is negligible (i.e., the bubble wall speed is much smaller than the sound speed inside the bubble), the system possesses spherical symmetry, effects due to vaporization, condensation, and surface tension, as well as variations in the temperature of the liquid are negligible and the thermal diffusion coefficient and the specific heats of the gas are constants.

We remind the reader that to model the bubble collapse and rebound, we simply study the evolution of our system when the initial radius $R(0)$ is much larger than the radius at equilibrium conditions $R_e (R(0) \gg R_e)$, the initial velocity of the bubble wall is $0\,(R_t(0) = 0)$ and the pressure in the liquid far away from the bubble remains at all times equal to the equilibrium pressure p_e.

Under these conditions, and introducing the change of variables

$$u = \frac{\rho}{\rho_g}\left(\frac{R}{R_e}\right)^3 \quad \text{and} \quad x = \frac{r}{R}, \tag{22}$$

the complete the complete set of equations governing the dynamics of our system reduces to the Rayleigh–Plesset equation

$$\rho_\ell\left(RR_{tt} + \frac{3}{2}R_t^2\right) + p_e = p_e\left(\frac{R_e}{R}\right)^3 u(x=1) \qquad R(0) = R_0, \quad R_t(0) = 0 \tag{23}$$

coupled with the nonlinear partial differential equation

$$u_t = \frac{(x^2 f)_x}{x^2} \qquad f(x=0) = f(x=1) = 0, \tag{24}$$

where f is given by

$$f = \left[\frac{1}{3\gamma}\frac{u_t(x=1)}{u(x=1)} + \frac{(\gamma-1)}{\gamma}\frac{R_t}{R}\right]xu + \frac{\lambda}{\gamma c_v \rho_g R_e^3} R\frac{u_x}{u}. \tag{25}$$

The system (22–25) was obtained independently by two different groups (see [30, 31] and [42, 43]). For completeness, we include its derivation in the Appendix D.

4.2. The asymptotic model

The fact that the initial bubble radius is much larger than the radius at equilibrium conditions ($R_0 \gg R_e$), makes it possible to solve the system (23–25) by means of asymptotic techniques. While this analysis is one of the main results of this paper, it can be somewhat technical for the reader not familiar with asymptotic methods. Thus, we have chosen to display and discuss the results here, and describe their derivation in the Appendix E.

The asymptotic behavior of the bubble radius as $\delta \to 0$ is given by

$$\frac{R(t)}{R_e} \sim \begin{cases} \delta^{-1} R_i(\tau) & \text{if} \quad \tau \le \tau_c \quad \text{and} \quad \delta^{\frac{10}{7}+\frac{5}{2(\gamma-1)}} \ll \tau_c - \tau \\ K\delta^{\frac{1}{(\gamma-1)}-\frac{3}{7}} R_a(\theta) & \text{if} \quad \theta \le 0 \quad \text{and} \quad -\theta \ll \delta^{-\frac{10}{7}-\frac{5}{2(\gamma-1)}}, \end{cases} \tag{26}$$

where R_i satisfies

$$R_i R_{i\tau\tau} + \tfrac{3}{2} R_{i\tau}^2 + 1 = 0 \qquad R_i(0) = 1, \quad R_{i\tau}(0) = 0; \tag{27}$$

R_a is the solution of

$$R_a R_{a\theta\theta} + \tfrac{3}{2} R_{a\theta}^2 = R_a^{-3\gamma} \qquad R_a(0) = \left(\frac{25}{6(\gamma-1)}\right)^{\frac{1}{3(\gamma-1)}}, \quad R_{a\theta}(0) = 0; \tag{28}$$

the parameter δ was defined in (5); τ is related to t through

$$t = R_0 \sqrt{\frac{\rho_\ell}{p_e}}\,\tau; \tag{29}$$

τ_c is the time at which R_i becomes 0 (i.e., $R_i(\tau_c) = 0$); θ is given by

$$\tau = a^{-\frac{5}{7} - \frac{25}{6(\gamma-1)}} b^{\frac{5}{6(\gamma-1)}} \mu^{-\frac{5}{7}} \delta^{\frac{10}{7} + \frac{5}{2(\gamma-1)}} \theta + \tau_c; \tag{30}$$

the constant b is defined in Appendix E; μ is given by (14); we have defined

$$a = \left(\frac{25}{6}\right)^{\frac{1}{5}} \tag{31}$$

and the constant K is given by

$$K = a^{\frac{5}{7} - \frac{5}{3(\gamma-1)}} b^{\frac{1}{3(\gamma-1)}} \mu^{-\frac{2}{7}}. \tag{32}$$

(We mention here that in the Appendix E we have used a different notation.) Formula (26) describes R for $t \in [0, t_{\min}]$, where $t_{\min}$ is the time at which R attains its minimum. Given our conditions, we have $R(t) = R(2t_{\min} - t)$ if $t_{\min} \le t \le 2t_{\min}$.

Our analysis provides us not only with the asymptotic form of the bubble radius R, but also with the asymptotic behavior of the other variables in the problem (such as density, pressure, and temperature of the gas, etc.). These expressions can be obtained following our analysis in the Appendix E. The constant b that appears in the above formulae, does not depend on δ. This constant has to be computed numerically and, when the thermal diffusion coefficient inside the bubble is constant, we obtained $b = 0.30$. If the thermal diffusion coefficient of the gas depends on the temperature, the value of b changes, but it is always an order 1 constant independent of δ.

Figure 4 shows plots of R/R_e versus t/t_e (t_e was defined in (4) and R is given by (26)) corresponding to the parameter values $\delta = 0.1$, $\mu = 0.5$, and $\gamma = 1.4$. We have plotted the inner and outer solutions. As expected the left plot looks exactly equal as the ones obtained in Section 2 with the polytropic approximations and in Section 3 with our informal model.

In agreement with our observations of Section 3, the analysis of Appendix E shows the presence of three different time scales in our problem. While the outer solution is valid (most of the time) the gas is isothermal and the bubble radius evolution is not affected by the gas pressure. For a shorter period of

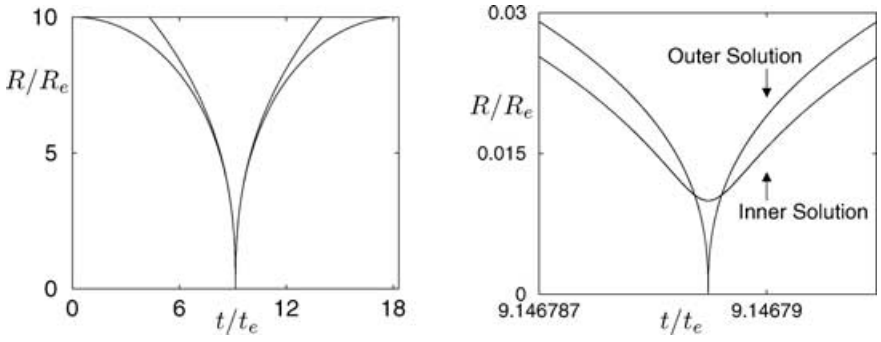

Figure 4. Plots R/R_e versus t/t_e corresponding to $\delta = 0.1$, $\gamma = 1.4$, and $\mu = 0.5$.

time, once the bubble has decreased in size substantially, the gas inside the bubble is neither isothermal nor adiabatic (the gas pressure does not affect the radius dynamics during this period). Finally, for a much shorter period, while the bubble is highly compressed, the gas is adiabatic and the pressure inside the bubble does affect the evolution of the radius, preventing it to become 0.

To compare the results of our asymptotics with the ones obtained in the previous sections, we remind that values of the minimum radius are $R_{\min} \approx 1.7 \times 10^{-144} R_e$ and $R_{\min} \approx 6.8 \times 10^{-3} R_e$ when the isothermal and adiabatic approximations are used respectively and $R_{\min} \approx 0.027 R_e$ when the informal approach of Section 3 is used (these values are obtained when $\delta = 0.1$, $\gamma = 1.4$, and $\mu = 0.5$). On the other hand, we show in the Appendix E that the asymptotic behavior of $R_{\min}$ as $\delta \to 0$ according to the present model (Equation (26)) is

$$R_{\min} \approx R_e \left(\frac{25}{6\mu^2} \right)^{\frac{1}{7}} \left(\frac{b}{\gamma - 1} \right)^{\frac{1}{3(\gamma-1)}} \delta^{\frac{1}{\gamma-1} - \frac{3}{7}}. \tag{33}$$

Thus, our asymptotic analysis gives $R_{\min} \approx 0.01 R_e$.

Note that our informal approach gave the right order of magnitude of $R_{\min}$ (compare Equations (21) and (33)). Also note the explicit dependence of our results on the parameters of the system (i.e., δ and μ). If we change our initial conditions or the fluids, we do not have to solve the Equations (27) and (28) again (unless γ changes). Another convenient feature of our approach is that the results obtained are easy to interpret, for example, formula (33) shows explicitly the dependence of $R_{\min}$ on δ and μ.

5. Applications, examples, and extensions

Thus far we have only considered a simple example in which we have a bubble collapse. In this Section we will show that the analysis of Section 4 can be applied to most situations where bubble collapses are relevant, and we will present two illustrative examples.

5.1. General applicability of the asymptotic expansions

In any situation (not only in the example of Section 4), while the bubble size decreases fast, the dynamics of the bubble radius is governed only by inertia (i.e., the first two terms of the Rayleigh–Plesset Equation (1)). Thus, during this period of time, R satisfies

$$R \sim A R_e t_e^{-\frac{2}{5}} (t_c - t)^{\frac{2}{5}} \tag{34}$$

for some constant A. The dimensionless constant A is large and depends on the history of the bubble evolution. This parameter A is a measure of the strength of the bubble collapse. In our example of Section 4, we have $A = (25/6)^{1/5}\delta^{-3/5}$.

For the short period of time while the bubble is highly compressed, its dynamics is independent of the pressure in the liquid at infinity. Thus, the asymptotic behavior of R during this short period of time depends only on A and it can be easily obtained from our analysis of Section 4 and Appendix E. We just have to replace $(25/6)^{1/5}\delta^{-3/5}$ by A. As a result, we obtain

$$R(t) \sim R_e A^{\frac{5}{7}-\frac{5}{3(\gamma-1)}} b^{\frac{1}{3(\gamma-1)}} \mu^{-\frac{2}{7}} R_a(\theta) \qquad \text{for } |\theta| \ll A^{\frac{5}{7}+\frac{25}{6(\gamma-1)}} \tag{35}$$

where R_a is the solution of (28) and θ is now given by

$$t = A^{-\frac{5}{7}-\frac{25}{6(\gamma-1)}} b^{\frac{5}{6(\gamma-1)}} \mu^{-\frac{5}{7}} t_e \theta + t_c. \tag{36}$$

In this sense our analysis is very general. The constant A of Equation (34) depends on the particular problem under consideration, but once A is obtained, the behavior of R while the bubble is highly compressed is given by Equations (35) and (36).

5.2. Slowly varying external pressure

We now illustrate our discussion with an example. More precisely, we will assume that the pressure in the liquid at infinity is not constant, but it is given by

$$p_\infty(t) = \begin{cases} p_e - p & \text{if } 0 < t < t_0 \\ p_e & \text{otherwise,} \end{cases} \tag{37}$$

where $p > p_e$, $t_0 \gg t_e$, $p/p_e - 1 = O(1)$ and the system is at equilibrium initially (i.e., $R(0) = R_e$ and $R_t(0) = 0$).

This external pressure p_∞ becomes negative at $t = 0$ and remains negative for a period of time t_0 much longer than t_e. Thus, the bubble size will be many times its equilibrium value by the time p_∞ becomes positive again ($t = t_0$) and as a consequence, the bubble will experience a collapse and rebound. In the

Appendix F we derive the asymptotic behavior of R for large values of t_0/t_e, obtaining

$$\frac{R(t)}{R_e} \sim \begin{cases} \varepsilon^{-1}\sqrt{\frac{2(p-p_e)}{3p_e}}\tau & \text{if} \quad \tau \leq 1 \quad \text{and} \quad \varepsilon \ll \tau \\ \varepsilon^{-1} R_i(\tau) & \text{if} \quad 1 \leq \tau \leq \tau_c \quad \text{and} \quad \varepsilon^{\frac{10}{7}+\frac{5}{2(\gamma-1)}} \ll \tau_c - \tau \\ K\varepsilon^{\frac{1}{(\gamma-1)}-\frac{3}{7}} R_a(\theta) & \text{if} \quad \theta \leq 0 \quad \text{and} \quad -\theta \ll \varepsilon^{-\frac{10}{7}-\frac{5}{2(\gamma-1)}}, \end{cases} \tag{38}$$

where R_i satisfies

$$R_i R_{i\tau\tau} + \frac{3}{2} R_{i\tau}^2 + 1 = 0 \qquad R_i(1) = R_{i\tau}(1) = \sqrt{\frac{2(p-p_e)}{3p_e}}; \tag{39}$$

R_a is the solution of (28); the parameter ε is defined as

$$\varepsilon = \frac{t_e}{t_0}; \tag{40}$$

τ is related to t through

$$t = t_0 \tau; \tag{41}$$

τ_c is the time at which R_i becomes 0 (i.e., $R_i(\tau_c) = 0$); θ is now given by

$$\tau = k^{-\frac{5}{7}-\frac{25}{6(\gamma-1)}} b^{\frac{5}{6(\gamma-1)}} \mu^{-\frac{5}{7}} \varepsilon^{\frac{10}{7}+\frac{5}{2(\gamma-1)}} \theta + \tau_c \tag{42}$$

(where $b = 0.30$ was defined in Appendix E and μ in (14)); k denotes the constant

$$k = \frac{9p - 5p_e}{8p_e}\sqrt{\frac{3}{2}}\left(\frac{p-p_e}{p_e}\right)^{\frac{3}{2}}; \tag{43}$$

and the constant K is now given by

$$K = k^{\frac{5}{7}-\frac{5}{3(\gamma-1)}} b^{\frac{1}{3(\gamma-1)}} \mu^{-\frac{2}{7}}. \tag{44}$$

(We mention here that in Appendix F we have used a different notation.) Figure 5 shows a plot of R/R_e versus t/t_e, where R is given by (38), $\varepsilon = 0.05$, $\gamma = 1.4$, and $\mu = 0.5$.

In this example, the strength of the bubble collapse is $A = k\varepsilon^{-3/5}$. In fact, it is easy to check that Equations (35) and (38) give the same results. This agrees with our previous discussion, namely, the calculation of the outer solution (and thus the constant A) depends on the particular problem under consideration, but the behavior of R in the boundary layer around its minimum is always given by (34–36). We remark that this example also illustrates another feature of our analysis that applies in general, namely, our asymptotics gives us the explicit dependence of the solution on the properties of the fluids and on the external pressure.

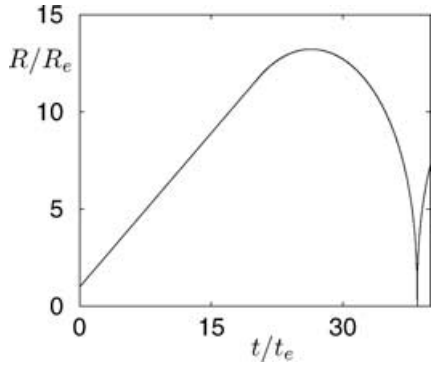

Figure 5. Plot R/R_e versus t/t_e where R is given by (38), $\mu = 0.5$, $\varepsilon = 0.05$, and $\gamma = 1.4$.

5.3. Two frequency forcing pressure

Bubble collapses can be easily produced by applying an acoustic field. The experiments in [20, 50] suggest that cavitation can be more efficiently induced if the acoustic field has two frequencies instead of one. Motivated by these experiments, we will consider the following example. We now assume that the pressure in the liquid at infinity is given by

$$p_\infty(t) = p_e(1 + a\sin(\omega t) + b\sin(2\omega t + \phi)). \tag{45}$$

Our goal is to find a, b, and ϕ that maximize the violence of the bubble collapses (and thus they also maximize the rate of chemical reactions that we want the cavitating bubbles to produce), given that the acoustic intensity and frequency are constant (i.e., $a^2 + b^2$ and ω are constants).

The first step toward the solution of this problem is to state it mathematically. This is naturally done thanks to our asymptotic analysis. Namely, the strength of the bubble collapse (the constant A of Equation (34)) is now a function of a, b, and ϕ. Thus, our problem is to maximize $A = A(a, b, \phi)$ under the restriction $a^2 + b^2 = r^2$, with r and ω constant. For convenience, we have parameterized a and b as $a = r\cos(\beta)$ and $b = r\sin(\beta)$. Thus, our problem in hand reduces to find β and ϕ that maximize A, i.e., solve the problem

$$A_{\max} = \max_{0\le\beta\le\frac{\pi}{2}} \bar{A}(\beta) \quad \text{where} \quad \bar{A}(\beta) = \max_{0\le\phi\le 2\pi} A(\beta, \phi). \tag{46}$$

For definiteness, we have used the values $r = 1.5p_e$ and $w = 0.05/t_e$. The calculation of $\bar{A}(\beta)$ and $A_{\max}$ is done in Appendix G. We found that $A_{\max} = 10.8$ and A is maximized at $\beta = 0.19\pi$ and $\phi = 0.4\pi$. Figure 6(a) shows a plot of $\bar{A}$ versus β. This plot clearly shows that the use of single frequency acoustic pressures is not optimal. Figure 6(b) shows a plot of R/R_e versus t/t_e when the external pressure is the one that maximizes A. Figure 6(c) shows a plot of this optimal pressure p_∞/p_e versus t/t_e. This plot shows that the valleys of p_∞ are

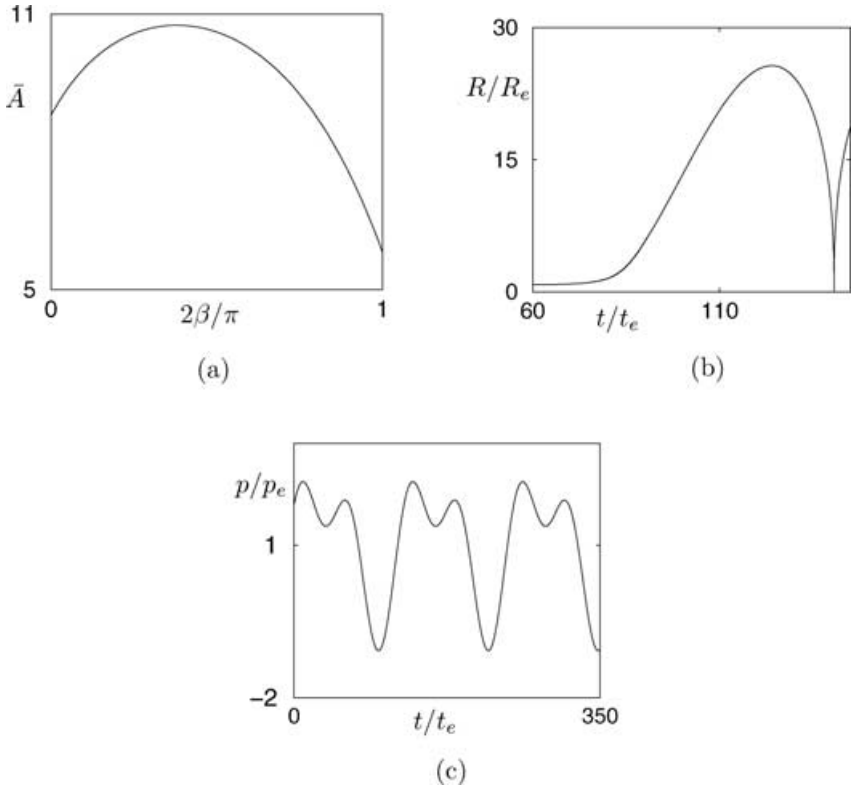

Figure 6. (a) Plot of $\bar{A}$ versus β (see Equation (46)). (b) Plot of R/R_e versus t/t_e when p_∞ is the one that maximizes A. (c) Plot of p_∞/p_e versus t/t_e

deep. This feature of p_∞ is expected, because the bubble growths while p_∞ is negative and thus, the longer p_∞ remains negative and the more negative it is, the larger the bubble is before it collapses and consequently the stronger it will collapse.

6. Discussion

We have shown that different models lead to extremely different results during a short but important period of time while the bubble is compressed.

We have quantified the strength of the bubble collapse by detecting a large nondimensional parameter (i.e., the constant A of Equation (34)) that is present whenever we are in the presence of a bubble collapse. We have presented two examples (one in Section 4 and the other one in Section 5.2) where we were able to find A analytically, but in general, the evaluation of A may require numerical computations. This was the case in our example of Section 5.3.

We have shown how to use this large parameter to simplify our system of equations with the use of asymptotic techniques. This asymptotic analysis

divides the time domain in 3 regions. The outer solution (while the bubble is expanded), depends on the particular problem under consideration. The other two regions in time correspond to two nested boundary layers around the time where the bubble radius attains its minimum. There, the evolution of the bubble radius is given by Equations (34–36) and the specific conditions of the particular problem under consideration enter only through the constant A.

We have discussed the general applicability and advantages of our method and we have also presented some illustrative examples. Our analysis can be extended to include effects neglected here (such as liquid compressibility). These extensions and applications of our method to the study of different problems where bubble collapses are relevant will be pursued in the future.

Appendix A: The isothermal and adiabatic approximations

In this appendix we derive the formulae in (6). To this end, we multiply equation (3) by R^2R_t and integrate once to obtain

$$\rho_\ell \frac{R^3R_t^2}{2} + p_e\frac{R^3}{3} = p_e\frac{R_0^3}{3} + p_eR_e^3\log\left(\frac{R}{R_0}\right) \tag{A.1}$$

and

$$\rho_\ell \frac{R^3R_t^2}{2} + p_e\frac{R^3}{3} + \frac{p_eR_e^3}{3(\gamma-1)}\left(\frac{R_e}{R}\right)^{3(\gamma-1)} = p_e\frac{R_0^3}{3} + \frac{p_eR_e^3}{3(\gamma-1)}\left(\frac{R_e}{R_0}\right)^{3(\gamma-1)} \tag{A.2}$$

in the isothermal and adiabatic case, respectively.

At the time where R attains its minimum, we have $R = R_{\min}$ and $R_t = 0$. Evaluating Equation (A.1) at this time, neglecting the left-hand side because $R_{\min} \ll R_0$, and using the identity $R_0 = R_e/\delta$, we immediately obtain the first formula in (6).

Similarly, replacing R by $R_{\min}$ and R_t by 0 in Equation (A.2) and, keeping only the third term of the left-hand side and the first term of the right-hand side (because the remaining terms are negligible in comparison), we obtain the second approximation in (6).

Appendix B: Collapse of an empty cavity

In this Appendix we derived the formula (11). We first multiply Equation (10) by R^2R_t and integrate the result to obtain

$$\rho_\ell \frac{R^3R_t^2}{2} + p_e\frac{R^3}{3} = p_e\frac{R_0^3}{3}. \tag{B.1}$$

Then we plug the ansatz $R = AR_et_e^{-\frac{2}{5}}(t_c - t)^\alpha$ into Equation (B.1) and take the limit $t \to t_c$ to conclude that $\alpha = 2/5$ and that A is given by (11).

Appendix C: Asymptotics on the informal model

In this Appendix we derive Equation (21). To do so we multiply Equation (19) by R^2R_t, integrate the result and use the information from the initial conditions (20) to obtain

$$\rho_\ell \frac{R^3R_t^2}{2} + p_e\frac{R^3}{3} + \frac{C}{3(\gamma-1)}R^{-3(\gamma-1)} \approx \rho_\ell \frac{R^3(t_\alpha)R_t^2(t_\alpha)}{2} = \frac{\rho_\ell}{3}R_e^5 t_e^{-2}\delta^{-3}. \tag{C.1}$$

In the derivation of this equation we have used the fact that both $p_eR^3(t_\alpha)$ and $CR^{-3(\gamma-1)}(t_\alpha)$ are much smaller than $\rho_\ell R^3(t_\alpha)R_t^2(t_\alpha)$. Finally, evaluating this expression at $R = R_{\min}$ and $R_t = 0$, and noticing that the first two terms of the left-hand side are negligible when R attains its minimum, we obtain Equation (21).

Appendix D: Derivation of the system (23–25)

In this Appendix we derive the system of equations (22–25). Under our assumptions (stated in Section 4), the complete set of Navier–Stokes equations (both in the liquid and the gas) reduce to the Rayleigh–Plesset equation

$$\rho_\ell\left(RR_{tt} + \tfrac{3}{2}R_t^2\right) + p_\infty(t) = p(t) \tag{D.1}$$

(where p_∞ is the pressure in the liquid at infinity) coupled with the conservation equations inside the bubble (this coupling is through the pressure in the bubble $p(t)$)

$$\rho_t + \frac{(r^2\rho v)_r}{r^2} = 0 \tag{D.2}$$

$$c_v\rho(T_t + vT_r) + \frac{(r^2v)_r}{r^2}p = \frac{\left(\lambda r^2T_r\right)_r}{r^2}. \tag{D.3}$$

Equations (D.2) and (D.3) are the conservation laws of mass and energy, respectively and we have not displayed the conservation of momentum because it reduces to $p_r = 0$ under the zero mach number approximation. Given that the gas is ideal, it satisfies the equation of state $p = \mathcal{R}\rho T$, where $\mathcal{R} = c_p - c_v = (\gamma-1)c_v$. This system of equations is completed once we prescribe the boundary conditions

$$T(r=R) = T_\ell \quad T_r(r=0) = 0 \quad v(r=R) = R_t, \tag{D.4}$$

where T_ℓ is the temperature of the liquid.

To derive the Equations (22–25), we make use of the equations of state and mass conservation, and the fact p is spatially uniform to rewrite the energy

equation as

$$p_t + \gamma \frac{(r^2 v)_r}{r^2} p = (\gamma - 1) \frac{\left(\lambda r^2 T_r\right)_r}{r^2}. \tag{D.5}$$

This equation can be integrated once to obtain the velocity as a function of the pressure and the temperature

$$v = \frac{(\gamma - 1)}{\gamma} \frac{\lambda T_r}{p} - \frac{r p_t}{3\gamma p}. \tag{D.6}$$

Using the equation of state and the boundary condition for the temperature $T(r = R) = T_\ell$ we can express the temperature and pressure inside the bubble as functions of the gas density

$$p = (\gamma - 1) c_v T_\ell \rho(r = R) \quad \text{and} \quad T = \frac{\rho(r = R)}{\rho} T_\ell. \tag{D.7}$$

Thus, we can now write the velocity as a function of the density

$$v = -\frac{\lambda \rho}{\gamma c_v \rho^2} - \frac{[\rho_t(r = R) + R_t \rho_r(r = R)]}{3\gamma \rho(r = R)} r. \tag{D.8}$$

Finally, plugging this expression for the velocity into the equation of conservation of mass and making the change of variables (22), we obtain, after some algebraic manipulations, the system (22–25).

Appendix E: Derivation of the asymptotic model of Section 4.2

In this Appendix we will reduce the set of Equations (23–25) to its asymptotic approximation. We will first introduce nondimensional variables. As a consequence, the parameter δ will appear in the dimensionless equations. The fact that δ is small, will naturally lead us to an asymptotic analysis. More precisely, we will introduce two nested boundary layers and as a result we will distinguish three regions in time. In a first region (where the outer solution is valid) the gas is isothermal and the evolution of the bubble radius is not affected by the pressure inside the bubble. A second region corresponds to a boundary layer in time where the isothermal approximation is no longer valid. And a third region corresponds to another boundary layer (inside the one where the gas is not isothermal) where the pressure inside the bubble affects the evolution of the bubble radius. We now proceed with the details of the analysis.

E.1. Outer solution: Isothermal behavior

Given the initial conditions, the choice of the dimensionless variables is natural:

$$R = R_0 \bar{R} \quad \text{and} \quad t = R_0 \sqrt{\frac{\rho_\ell}{p_e}} \bar{t}. \tag{E.1}$$

In these new variables, our system (23–25) becomes

$$\bar{R}\bar{R}_{\bar{t}\bar{t}} + \tfrac{3}{2}\bar{R}_{\bar{t}}^2 + 1 = \delta^3 \bar{R}^{-3} u(x=1) \qquad \bar{R}(0) = 1 \quad \text{and} \quad \bar{R}_{\bar{t}} = 0 \tag{E.2}$$

and

$$u_{\bar{t}} = \frac{(x^2 \bar{f})_x}{x^2} \qquad \bar{f}(x=0) = \bar{f}(x=1) = 0, \tag{E.3}$$

where $\bar{f}$ is given by

$$\bar{f} = \left[\frac{1}{3\gamma} \frac{u_{\bar{t}}(x=1)}{u(x=1)} + \frac{(\gamma-1)}{\gamma} \frac{\bar{R}_{\bar{t}}}{\bar{R}} \right] xu + \frac{\mu}{\gamma \delta^2} \bar{R} \frac{u_x}{u}. \tag{E.4}$$

As previously mentioned, we will assume that μ is a parameter of order 1 and δ is small. Thus, we can simplify our system (E.2–E.4) by keeping only the dominant terms. More precisely, we approximate $\bar{R}$ and u by $\bar{R}_0$ and u_0, respectively, where these new variables satisfy

$$\bar{R}_0 \bar{R}_{0\bar{t}\bar{t}} + \tfrac{3}{2}\bar{R}_{0\bar{t}}^2 + 1 = 0 \qquad \bar{R}_0(0) = 1 \quad \text{and} \quad \bar{R}_{0\bar{t}} = 0 \tag{E.5}$$

and

$$0 = \left(x^2 \frac{u_{0x}}{u_0} \right)_x \quad \text{with} \quad u_{0x}(x=0) = u_{0x}(x=1) = 0. \tag{E.6}$$

From this last equation we infer that u_0 is a constant and, going back to the relation between u and the gas density (Equation (22)), we immediately conclude that this constant should be 1

$$u \sim u_0 = 1. \tag{E.7}$$

On the other hand, as already discussed in Section 3, $\bar{R}_0$ decreases monotonically, it becomes 0 at a finite time $\bar{t}_c$ and the asymptotic behavior of $\bar{R}_0$ as $\bar{t}$ approaches $\bar{t}_c$ is given by

$$\bar{R}_0 \sim a(\bar{t}_c - \bar{t})^{\frac{2}{5}}, \quad \text{where} \quad a = \left(\frac{25}{6} \right)^{\frac{1}{5}}. \tag{E.8}$$

E.2. Boundary layer: Failure of the isothermal approximation

As the bubble becomes small, the approximation (E.4) fails because some neglected effects become important. To take these effects into account, we need to introduce a boundary layer in time. Let α be the boundary layer thickness (α is yet to be determined). Then, given the equation (E.8), we introduce the change of variables.

$$\bar{R} = a\alpha^{\frac{2}{5}} \hat{R} \quad \text{and} \quad \bar{t} = \bar{t}_c + \alpha \hat{t}. \tag{E.9}$$

Thus, plugging these expressions into equations (E.2–E.4), our system becomes

$$\hat{R}\hat{R}_{\hat{t}\hat{t}} + \tfrac{3}{2}\hat{R}_{\hat{t}}^2 + a^{-2}\alpha^{\frac{6}{5}} = a^{-5}\delta^3 \hat{R}^{-3} u(x=1) \tag{E.10}$$

and

$$u_{\hat{t}} = \frac{(x^2 \hat{f})_x}{x^2} \qquad \hat{f}(x=0) = \hat{f}(x=1) = 0, \tag{E.11}$$

where

$$\hat{f} = \left[\frac{1}{3\gamma} \frac{u_{\hat{t}}(x=1)}{u(x=1)} + \frac{(\gamma-1)}{\gamma} \frac{\hat{R}_{\hat{t}}}{\hat{R}} \right] xu + \frac{a\mu}{\gamma \delta^2} \alpha^{\frac{7}{5}} \hat{R} \frac{u_x}{u}. \tag{E.12}$$

From these equations it is clear that the approximation for u (equation (E.7)) is the first one to fail. This fact leads us to the natural choice of α that makes the coefficient multiplying $\hat{R}u_x/u$ in the formula (E.12) an order one quantity

$$\alpha = \left[\frac{\delta^2}{a\mu} \right]^{5/7}. \tag{E.13}$$

To solve (E.10), note that a is an order one constant and both δ and α are small parameters. Then, neglecting the small terms in Equation (E.10) (i.e., we only keep the first two terms of the left-hand side), solving for $\hat{R}$ and matching the result with the outer solution, we obtain the asymptotic behavior of $\hat{R}$ (for small values of δ)

$$\hat{R} \sim (-\hat{t})^{2/5} \qquad \text{(for negative } \hat{t}\text{)}. \tag{E.14}$$

This approximation fails as $\hat{t} \to 0$. Thus, we will need to include a new boundary layer. To this end, we first need to study the behavior of u as $\hat{t}$ goes to 0. In this limit, the motion becomes adiabatic. This means that the pressure becomes proportional to $R^{-3\gamma}$ and the entropy becomes constant along particle paths. These facts and the asymptotic behavior of $\hat{R}$ (Equation (E.14)) imply that u satisfies

$$u(x=1) \sim b(-\hat{t})^{-\frac{6(\gamma-1)}{5}} \quad \text{and} \quad u \sim u_0(x) \quad (\text{for } x \neq 1 \text{) as} \quad \hat{t} \to 0 \tag{E.15}$$

for some constant b and some function $u_0(x)$. To compute the constant b and the function u_0, we need to replace $\hat{R}$ by its asymptotic approximation $(-\hat{t})^{2/5}$ in Equation (E.11) and solve that equation with u subject to the asymptotic behavior $u \sim 1$ as $\hat{t} \to -\infty$. We have computed b numerically and we obtained

$$b = 0.30 \tag{E.16}$$

(The details of the numerical code to compute b and $u_0(x)$ will not be discussed here).

E.3. Thinner boundary layer: Adiabatic behavior

Equations (E.14) and (E.15) imply that the right-hand side of (E.10) becomes of the same order of the left-hand side of that equation when $\hat{t} = O(\delta^{5/(2(\gamma-1))})$ and thus, the approximation used to obtained (E.14) fails for such small values

of $\hat{t}$. Consequently, we need to introduce a new boundary layer (inside the one we already have). To do so we define

$$\beta = (\delta^3 b a^{-5})^{\frac{5}{6(\gamma-1)}} \tag{E.17}$$

and make the change of variables

$$\hat{R} = \beta^{2/5}\tilde{R}, \quad \hat{t} = \beta\tilde{t} \tag{E.18}$$

and, for convenience, we introduce the function $h(\tilde{t})$ defined by

$$u(x=1) = b\beta^{-\frac{6}{5}(\gamma-1)}h. \tag{E.19}$$

Equations (E.15–E.17) now become

$$\tilde{R}\tilde{R}_{\tilde{t}\tilde{t}} + \tfrac{3}{2}\tilde{R}_{\tilde{t}}^2 + a^{-2}(\alpha\beta)^{\frac{6}{5}} = \tilde{R}^{-3}h \tag{E.20}$$

$$u_{\tilde{t}} = \frac{(x^2\tilde{f})_x}{x^2} \quad \tilde{f}(x=0) = \tilde{f}(x=1) = 0 \tag{E.21}$$

$$\tilde{f} = \left[\frac{1}{3\gamma}\frac{h_{\tilde{t}}}{h} + \frac{(\gamma-1)}{\gamma}\frac{\tilde{R}_{\tilde{t}}}{\tilde{R}}\right]xu + \frac{\beta^{\frac{7}{5}}}{\gamma}\tilde{R}\frac{u_x}{u}. \tag{E.22}$$

Thus, matching the solutions in both boundary layers as $\tilde{t}$ goes to $-\infty$ and $\hat{t}$ goes to 0 and neglecting the small terms in (E.20–E.22) we obtain the following approximations for $\tilde{R}$ and u

$$\tilde{R} \sim \tilde{R}_0, \quad u \sim u_0(x) \quad \text{and} \quad \tilde{h} \sim \tilde{R}_0^{-3(\gamma-1)} \tag{E.23}$$

where $\tilde{R}_0$ satisfies

$$\tilde{R}_0\tilde{R}_{0\tilde{t}\tilde{t}} + \tfrac{3}{2}\tilde{R}_{0\tilde{t}}^2 = \tilde{R}_0^{-3\gamma} \quad \text{and} \quad \tilde{R}_0 \sim (-\tilde{t})^{2/5} \quad \text{as} \quad \tilde{t} \to -\infty. \tag{E.24}$$

Note that the asymptotic behavior of $\tilde{R}_0$ does not uniquely determine $\tilde{R}_0$. To implement our results, it is convenient to have $\tilde{R}_0$ uniquely determined and have initial conditions instead of its asymptotic behavior. Thus, we arbitrarily choose $\tilde{R}_{0\tilde{t}}(0) = 0$ and to determine $\tilde{R}_0(0)$, we note that

$$E(\tilde{t}) = \frac{\tilde{R}_0^3\tilde{R}_{0\tilde{t}}^2}{2} + \frac{\tilde{R}_0^{3(\gamma-1)}}{3(\gamma-1)} \tag{E.25}$$

is constant and consequently $E(0) = E(-\infty)$ from where $\tilde{R}_0(0)$ can be obtained. In summary, $\tilde{R}_0$ satisfies

$$\tilde{R}_0\tilde{R}_{0\tilde{t}\tilde{t}} + \frac{3}{2}\tilde{R}_{0\tilde{t}}^2 = \tilde{R}_0^{-3\gamma} \qquad \tilde{R}_0(0) = \left(\frac{25}{6(\gamma-1)}\right)^{\frac{1}{3(\gamma-1)}} \text{ and } \tilde{R}_{0\tilde{t}}(0) = 0, \tag{E.26}$$

which completes our asymptotic analysis.

Appendix F: Asymptotics for the example of Section 5.2

In this Appendix we show how to extend our asymptotic analysis to the case in which the external pressure is given by (37) and the initial conditions are $R(0) = R_e$ and $R_t(0) = 0$. The equations to solve now are

$$\rho_\ell \left(RR_{tt} + \frac{3}{2} R_t^2 \right) + p_\infty(t) = p_e \left(\tfrac{R_e}{R}\right)^3 u(x=1); \qquad R(0) = R_e, \quad R_t(0) = 0 \tag{F.1}$$

and equations (24–25). Our first step is to nondimensionalize these equations. Given the external pressure, the natural choice of the dimensionless variables is

$$t = t_0 \bar{t} = \frac{t_e}{\varepsilon} \bar{t} \quad \text{and} \quad R = t_0 \sqrt{\frac{p_e}{\rho_\ell}} \bar{R} = \frac{R_e}{\varepsilon} \bar{R}, \tag{F.2}$$

where we have introduced the notation

$$\varepsilon = \frac{t_e}{t_0}. \tag{F.3}$$

Thus our system becomes

$$\bar{R} \bar{R}_{\bar{t}\bar{t}} + \frac{3}{2} \bar{R}_{\bar{t}}^2 + \frac{p_\infty}{p_e} = \varepsilon^3 \frac{u(x=1)}{\bar{R}^3} \qquad \bar{R}(0) = \varepsilon \quad \text{and} \quad \bar{R}_{\bar{t}}(0) = 0 \tag{F.4}$$

and

$$u_{\bar{t}} = \frac{(x^2 \bar{f})_x}{x^2} \qquad \bar{f}(x=0) = \bar{f}(x=1) = 0 \tag{F.5}$$

where $\bar{f}$ is given by

$$\bar{f} = \left[\frac{1}{3\gamma} \frac{u_{\bar{t}}(x=1)}{u(x=1)} + \frac{(\gamma - 1)}{\gamma} \frac{\bar{R}_{\bar{t}}}{\bar{R}} \right] xu + \frac{\mu}{\gamma \varepsilon^2} \frac{u_x}{u}. \tag{F.6}$$

A simply asymptotic analysis with ε as the small expansion parameter, shows that

$$\bar{R} \sim \sqrt{\frac{2(p - p_e)}{3p_e}} \bar{t} \quad \text{and} \quad u \sim 1 \text{ for } \varepsilon \ll \bar{t} \leq 1. \tag{F.7}$$

To solve these equations for $\bar{t} > 1$, we follow similar arguments of Appendix E. We approximate $\bar{R}$ and u by $\bar{R}_0$ and u_0 respectively, where these new variables satisfy

$$\bar{R}_0 \bar{R}_{0\bar{t}\bar{t}} + \frac{3}{2} \bar{R}_{0\bar{t}}^2 + 1 = 0 \qquad \bar{R}_0(1) = \bar{R}_{0\bar{t}}(1) = \sqrt{\frac{2(p - p_e)}{3p_e}} \tag{F.8}$$

and

$$0 = \left(x^2 \frac{u_{0x}}{u_0} \right)_x \quad \text{with} \quad u_{0x}(x=0) = u_{0x}(x=1) = 0. \tag{F.9}$$

Equation (F.9) implies

$$u \sim u_0 = 1. \tag{F.10}$$

On the other hand, $\bar{R}_0$ becomes 0 at a finite time $\bar{t}_0$ and the asymptotic behavior of $\bar{R}_0$ as $\bar{t}$ approaches $\bar{t}_0$ is now given by

$$\bar{R}_0 \sim k(\bar{t}_0 - \bar{t})^{\frac{2}{5}} \qquad \text{where} \quad k = \frac{9p - 5p_e}{8p_e} \sqrt{\frac{3}{2}} \left(\frac{p - p_e}{p_e} \right)^{\frac{3}{2}}. \tag{F.11}$$

To obtain k, we used the fact that

$$E(\bar{t}) = \frac{\bar{R}_0^3 \bar{R}_{0\bar{t}}^2}{2} + \frac{\bar{R}_0^3}{3} \tag{F.12}$$

is constant and thus, k can be obtained from the equation $E(1) = E(\bar{t}_0)$. Note that we are now in exactly the same situation as in the Appendix E once we replace δ by ε and the constant a of equation (E.8) by k (see Equation (F.11)). Thus, the remaining asymptotic analysis follows from that Appendix.

Appendix G: Asymptotics for the example of Section 5.3

In this Appendix we complete the calculations of Section 5.3.

G.1. Positive slowly varying external pressure

If the external pressure p_∞ is positive and varies slowly (i.e., $p_\infty = p_\infty(\omega t)$ with $\omega t_e \ll 1$) and the initial radius $R(0)$ is of the order of the equilibrium radius R_e, the bubble will behave *quasitalically* after a transient time of the order t_e. More precisely, the gas will be isothermal and the bubble radius will approximately satisfy

$$p_\infty(\omega t) = p_e \left(\frac{R_e}{R} \right)^3. \tag{G.1}$$

G.2. Nonpositive slowly varying external pressure

Suppose now that p_∞ is of the form $p_\infty = p_\infty(\omega t)$ with $\omega t_e \ll 1$ and that p_∞ is positive for t satisfying $0 < t < t_0$ or $t_1 < t$ but it is negative for t in the time interval (t_0, t_1). In this case, the bubble radius will satisfy (G.1) for $0 < t < t_0$, but for larger values of t the bubble will grow. If we further assume that $\omega(t_1 - t_0) = 0(1)$ and that the minimum of p_∞ is of the order of p_e, the evolution of R for $t > t_0$ can be described follows.

We first introduce the dimensionless variables

$$\tau = \omega t = \varepsilon \frac{t}{t_e} \quad \text{and} \quad R_i = \varepsilon \frac{R}{R_e}. \tag{G.2}$$

where $\varepsilon = \omega t_e$. The Rayleigh–Plesset equation (see (23)) now becomes

$$R_i R_{i\tau\tau} + \frac{3}{2} R_{i\tau}^2 + P(\tau) = \varepsilon^3 \frac{u(x=1)}{R_i^3}, \tag{G.3}$$

where $P(\tau) = p_\infty(\tau)/p_e$. Since $\varepsilon \ll 1$, we neglect the right-hand side of (G.3). To find the initial conditions of R_i at $\tau = \tau_0 = \omega t_0$, we need to match the behavior of R for $t < t_0$ (Equation (G.1)) and $t_0 < t$. Clearly, in the limit of small values of ε, this matching leads to the initial conditions $R_i(\tau_0) = R_{i\tau}(\tau_0) = 0$. In summary, in the limit $\varepsilon \to 0$, the asymptotic behavior of the bubble radius is given by

$$R_i R_{i\tau\tau} + \tfrac{3}{2} R_{i\tau}^2 + P(\tau) = 0 \quad \text{and} \quad R_i(\tau_0) = R_{i\tau}(\tau_0) = 0. \tag{G.4}$$

for $\tau > \tau_0$.

Since P becomes positive, R_i eventually becomes 0 at a finite time $\tau = \tau_c$. In fact, the behavior of R_i as $\tau \to \tau_c$ is given by

$$R_i \sim B(\tau_c - \tau)^{\frac{2}{5}} \tag{G.5}$$

for some constant B. In other words, if we define $t_c = \tau_c/\omega$, the asymptotic behavior of R as $t \to t_c$ in the limit $\omega t_e \to 0$ is

$$R \sim A R_e t_e^{-\frac{2}{5}} (t_c - t)^{\frac{2}{5}}, \tag{G.6}$$

where the constants B and A of equations (G.5) and (G.6), respectively are related by

$$A = \varepsilon^{-3/5} B. \tag{G.7}$$

It is clear that this constant B depends only on $P(\tau)$.

G.3. Slowly varying two frequency external pressure

We are now ready specialize our analysis to the example of Section 5.3. Namely, we set $P(\tau) = 1 + a\sin(\tau) + b\cos(2\tau + \phi)$, where $a = r\cos(\beta)$ and $b = r\sin(\beta)$, we choose $r = 1.5$ and $\varepsilon = 0.05$ and we now follow the procedure described above to compute $A = A(\beta, \phi)$ numerically.

References

1. B. P. Barber, R. A. Hiller, R. Lofstedt, S. J. Putterman, and K. R. Weninger, Defining the unknowns of sonoluminescence, *Phys. Rep.* 281:66–143 (1997).
2. B. P. Barber and S. J. Putterman, Observations of synchronous picoseconds sonoluminescence, *Nature* 352:318–320 (1991).

3. B. P. Barber, K. Arisaka, H. Fetterman, and S. J. Putterman, Resolving the picoseconds characteristics of synchronous sonoluminescence, *J. Acoust. Soc. Am.* 91:3061–3063 (1992).
4. C. E. Brennen, *Cavitation and bubble dynamics*, Oxford University Press, Oxford, 1995.
5. M. P. Brenner, S. Hilgenfeldt, and D. Lohse, Single-bubble sonoluminescence, *Rev. Mod. Phys.* 74:425–484 (2002).
6. A. Eller, Growth of bubbles by rectified diffusion, *J. Acoust. Soc. Am.* 46:1246–1250 (1969).
7. A. Eller and L. Crum, Instability of motion of a pulsating bubble in a sound field, *J. Acoust. Soc. Am.* 47:762 (1970).
8. A. Eller and H. G. Flynn, Rectified diffusion during nonlinear pulsations of cavitation bubbles, *J. Acoust. Soc. Am.* 37:493–503 (1964).
9. P. S. Epstein and M. S. Plesset, On the stability of gas bubbles in liquid–gas solutions, *J. Chem. Phys.* 18:1505 (1950).
10. H. Frenzel and H. Schultes, Lumineszenz imultraschall–beschickten Wasser, *Z. Phys. Chem. Abstr. B* 27:421–424 (1934).
11. D. F. Gaitan, L. A. Crum, C. C. Church, and R. A. Roy, Sonoluminescence and bubble dynamics for a single, stable, cavitation bubble, *J. Acoust. Soc. Am.* 91:3166–3183 (1992).
12. P. T. Greenland, Sonoluminescence, *Contemp. Phys.* 40:11–30 (1999).
13. H. P. Greenspan and A. Nadim, On sonoluminescence of an oscillating gas bubble, *Phys. Fluids A* 5:1065–1067 (1993).
14. R. Hiller, K. Weninger, S. J. Putterman, and B. P. Barber, Effect on noble-gas doping in single-bubble sonoluminescence, *Science* 266:248–250 (1994).
15. G. Iernetti, N. V. Dezhkunov, M. Reali, A. Francescutto, and G. K. Johri, Enhancement of high-frequency acoustic cavitation effects by low-frequency simulation, *Ultrason. Sonochem.* 4:263–268 (1997).
16. V. Kamath, H. N. Oguz, and A. Prosperetti, Bubble oscillations in the nearly adiabatic limit, *J. Acoust. Soc. Am.* 92:2016–2023 (1992).
17. V. Kamath, A. Prosperetti, and F. N. Egolfopoulos, A theoretical study of sonoluminescence, *J. Acoust. Soc. Am.* 94:248–260 (1993).
18. K. Kawabata and S. Umemura, Use of second-harmonic superimposition to induce chemical effects of ultrasound, *J. Phys. Chem.* 100:18784–18789 (1996).
19. H. Y. Kwak and J. H. Na, Physical processes for single bubble sonoluminescence, *J. Phys. Soc. Japan* 66:3074–3083 (1997).
20. H. Y. Kwak and H. Yang, An aspect of sonoluminescence from hydrodynamic theory, *J. Phys. Soc. Japan* 64:1980–1992 (1995).
21. T. G. Leighton, *The Acoustic Bubble*, Academic, London, 1994.
22. H. Lin, B. D. Storey, and A. J. Szeri, Inertially driven inhomogeneities in violently collapsing bubbles: The validity of the Rayleigh–Plesset equation, *J. Fluid Mech.* 452:145–162 (2002).
23. H. Lin and A. J. Szeri, Rayleigh–Taylor instability of violently collapsing bubbles, *Phys. Fluids* 14:2925–2928 (2002).
24. H. Lin and A. J. Szeri, Shock formation in the presence of entropy gradients, *J. Fluid Mech.* 431:161–188 (2001).
25. T. J. Mason and J. P. Lorimer, *Sonochemistry: Theory, Applications and Uses of Ultrasound in Chemistry*, Wiley, New York, 1988.

26. T. J. Mason, *Sonochemistry*, Oxford University Press, Oxford, 1999.
27. W. C. Moss, D. B. Clarke, J. W. White, and D. A. Young, Hydrodynamic simulations of bubble collapse and picosecond sonoluminescence, *Phys. Fluids* 6:2979–2985 (1994).
28. F. B. Nagiev and N. S. Khabbev, Heat transfer and phase-transition effects associated with oscillations of vapor–gas bubbles, *Sov. Phys. Acoust.* 25:148–152 (1979).
29. R. I. Nigmatulin, N. S. Khabeev, and F. B. Nagiev, Dynamics, heat and mass transfer of vapor–gas bubbles in a liquid, *Int. J. Heat Mass Transfer* 24:1033–1043 (1981).
30. E. A. Neppiras, Acoustic cavitation, *Phys. Rep.* 61:159–251 (1980).
31. M. Plesset, The dynamics of cavitation bubbles, *J. Appl. Mech.* 16:277 (1949).
32. M. Plesset, On the stability of fluid flows with spherical symmetry, *J. Appl. Phys.* 25:96 (1954).
33. M. Plesset and T. P. Mitchell, On the stability of the spherical shape of a vapor cavity in a liquid, *Q. Appl. Math.* 13:419–430 (1956).
34. M. Plesset and A. Prosperetti, Bubble dynamics and cavitation, *Annu. Rev. Fluid Mech.* 9:145–185 (1977).
35. M. Plesset and S. A. Zwick, The growth of vapor bubbles in superheated liquids, *J. Appl. Phys.* 23:95 (1952).
36. A. Prosperetti, Nonlinear oscillations of gas bubbles in liquids: Steady-state solutions, *J. Acoust. Soc. Am.* 56:878–885 (1974).
37. A. Prosperetti, Nonlinear oscillations of gas bubbles in liquids: Transient solutions and the connection between sub-harmonic signal and cavitation, *J. Acoust. Soc. Am.* 57:810–821 (1975).
38. A. Prosperetti, Current topics in the dynamics of gas and vapor bubbles, *Meccanica* 12:214–235 (1977).
39. A. Prosperetti, Viscous effects on perturbed spherical flows, *Q. Appl. Math.* 34:339–350 (1977).
40. A. Prosperetti, The thermal behavior of oscillating gas bubbles, *J. Fluid Mech.* 222:587–616 (1991).
41. A. Prosperetti, L. A. Crum, and K. W. Commander, Nonlinear bubble dynamics, *J. Acoust. Soc. Am.* 83:502–514 (1988).
42. A. Prosperetti and Y. Hao, Modelling of spherical gas bubble oscillations and sonoluminescence, *Phil. Trans. Royal Soc. London A* 357:203–223 (1999).
43. A. Prosperetti and A. Lezzi, Bubble dynamics in a compressible liquid, *J. Fluid Mech.* 168:457–478 (1986).
44. S. J. Putterman and K. R. Weninger, Sonoluminescence: How bubbles turn sound into light, *Annu. Rev. Fluid Mech.* 32:445–476 (2000).
45. L. Rayleigh, On the pressure developed in a liquid during the collapse of a spherical cavity, *Phil. Mag.* 34:94–98 (1917).
46. B. D. Storey and A. J. Szeri, A reduced model of cavitation physics for use in sonochemistry, *Proc. Royal Soc. London A* 457:1685–1700 (2001).
47. K. S. Suslick and G. J. Price, Applications of ultrasound to materials chemistry, *Annu. Rev. Mater. Sci.* 29:295–326 (1999).
48. S. Umemura, K. Kawabata, K. Sasaki, N. Yumita, K. Umemura and R. Nishigaki, Recent advances in sonodynamic approach to cancer therapy, *Ultrasonics Sonochem.* 3:187–191 (1996).

49. V. Q. Vuong, A. J. Szeri, and D. A. Young, Shock formation within sonoluminescence bubbles, *Phys. Fluids* 11:10–17 (1999).
50. A. J. Walton and G. T. Reynolds, Sonoluminescence, *Adv. Phys.* 33:595–600 (1984).
51. F. R. Young, *Cavitation*, Mc Graw-Hill Book Company, New York, 1989.

Georgia Institute of Technology

(Received November 27, 2002)